Desalination and Water Treatment
www.deswater.com

doi: 10.1080/19443994.2013.838523

53 (2015) 452–461
January

Taylor & Francis
Taylor & Francis Group

Development of olivestones-activated carbons by physical, chemical and physicochemical methods for phenol removal: a comparative study

L. Temdrara[a]*, A. Addoun[b], A. Khelifi[b]

[a]*Faculté des Sciences, Université Hassiba Benbouali de Chlef, BP 151, 02000 Chlef, Algerie*
Tel. +213 662923830; email: temlarbi@yahoo.fr
[b]*Faculté de Chimie, USTHB, BP 32, El-Alia, 16111 Bab-Ezzouar, Alger, Algeria*

Received 16 April 2013; Accepted 23 August 2013

ABSTRACT

Olive stones, an agricultural waste, have successively undergone a chemical activation by $ZnCl_2$ (coals CZ), a physical activation by CO_2 (coals CP) and a combined activation by $ZnCl_2$ followed by CO_2 (coals CC) in order to compare the efficiency of these activating agents in the production of activated carbons for their applications in polluted water treatment. The obtained results show that the larger the ratio of $ZnCl_2$ to olive stones (coals CZ and CC), and the duration of preservation of CO_2 (coals CP), the more developed the porous texture. These results are confirmed by immersion calorimetry in cyclohexane and tri-2,4-xilyl phosphate. The adsorption of phenol in aqueous solution on all activated carbons at 25°C was investigated. The adsorption kinetics data were well described by the pseudo-second-order model, and all phenol adsorption isotherms on various activated carbons perfectly fit the Langmuir equation. Furthermore, the phenol adsorption capacities of activated carbons obtained by physical and physicochemical activations successively (CP3 and CC3) were the largest (156 and 158 mg/g, respectively) although the specific surface area (S_{BET}) of CP3 (861 m^2/g) is much lower than that of CC3 (1793 m^2/g); this should be due to the presence of narrower microporosity in the activated carbons CC. The best activated carbon, in terms of the porous texture (specific surface area and total pore volume), is the one obtained by physicochemical activation (CC3).

Keywords: Activated carbon; Adsorption; Phenol; Combined activation

1. Introduction

Manufacturing activated carbons involves two steps: the carbonization of raw carbonaceous materials in an inert atmosphere and the activation of carbonized product. The carbonization consists of a thermal decomposition of the carbonaceous material, eliminating non-carbon species and producing a fixed carbon mass with a rudimentary pore structure. Very fine and closed pores are created during this step, the purpose of activation is to enlarge the diameters of the fine pores and create new pores.

The activation can be carried out by chemical or physical means. In chemical activation, the carbonization and activation are accomplished in a single step by carrying out decomposition of the raw

*Corresponding author.

material impregnated with certain chemical agents. The advantages of chemical activation are their low energy cost due to lower temperatures than those needed for physical activation, and high product yields.

The physical activation involves gasification of the char (obtained from carbonization of the raw material) by oxidizing with steam, carbon dioxide, air or any mixture of these gases in the temperature range 800 to 1,100°C.

Activated carbons with high apparent surface areas and pore volume were obtained from treatments of lignocellulosics precursors with phosphoric acid and zinc chloride [1–3]. The zinc chloride is one of the chemical activating agents used in the preparation of activated carbon [4–11]. The formation of highly microporous carbons by pyrolysis of various types of precursors (lignocellulosic materials, green cokes, and coals) in presence of potassium and sodium hydroxides and carbonates is now well documented [12–15]. Alkaline and carbonate hydroxides and carbonate potassium were also used in the chemical activation of coals [14,16].

For a long time, activated carbons have been widely used for the removal of organic pollutants from wastewaters and drinking water, due to their large surface area and pore volume [17]. Currently, around 275,000 tons of activated carbons are consumed annually worldwide [18]. Because of the high cost and non-renewable source of commercially available activated carbon, in recent years, researchers have studied the production of activated carbons from low cost [19] and renewable resources, such as coconut husk, wood, date stones, coffee endocarp, bamboo, cotton stalks, pistachio shell, and olive stones. Olive-waste cakes, corresponding to the remaining residue of oil extraction process, represent a yearly average of 15 million tons depending on the crop [20].

Phenol is a common pollutant in municipal water and industrial effluents. Adsorption is one of the most effective processes for the removal of phenol [21–26]. The phenomenon of heat released during the immersion of a solid in a liquid, with which it does not react and in which it does not dissolve, is obviously due to the solid–liquid interaction and corresponds to the heat of immersion of the solid. The released heat quantities reflect the interaction forces between the liquid molecules and the solid, which determine the adsorption degree. The calorimetry of immersion was used in the characterization of the carbon materials: porous texture [27–30], pore size distribution from their enthalpies of immersion in liquids of different molecular dimensions [30,31], free energy [32], and polarity of surface [32,33].

The objective of this study relates to the valorization of a lignocellulosic compound, the olive stones, and an agricultural waste. For this purpose, the raw material was successively chemically activated by zinc chloride, physically activated by carbon dioxide, and activated by zinc chloride followed by carbon dioxide (combined activation) in order to produce activated carbons with high surface areas and pore volume for their application in the polluted water treatment.

2. Experimental

2.1. Preparation of activated carbons

The olive stones were beforehand oven-dried at 120°C before being crushed and sieved until obtaining a granulometry lower than 0.315 mm (powder) to improve the contact between the activating agent and lignocellulosic material. They are again dried at 120°C and kept in hermetically closed flasks.

For the chemical activation, the homogeneous mixture (olive stones and zinc chloride) was carbonized in a horizontal furnace under a nitrogen flow of $100\,cm^3\,min^{-1}$ with a heating rate of 5°C/min from room temperature to the final temperature (800°C) and maintained for one hour at this temperature, in order to have the same temperature for the physical activation, before cooling. After cooling under a nitrogen flow, the obtained carbon was treated by an hydrochloric acid solution (0.1 N) by refluxing for three hours, then washed with boiling distilled water until the absence of chloride ions, and finally oven-dried at 120°C for three hours and kept in hermetic bottles to protect it from air and humidity. The olive stones activated with various ratio of $ZnCl_2$ (0.5 g, 1 g and 2 g) were denoted as CZ1, CZ2 and CZ3, respectively.

In relation to physical activation, the powder of olive stones was carbonized in the same conditions as previously (without landing of 1 h); the nitrogen is then substituted by the carbon dioxide in various durations (1, 2, and 3 h); after cooling under a nitrogen flow, the obtained material was washed in distilled water. We shall note that CP1, CP2, and CP3 coals were treated for 1, 2 and 3 h with CO_2, respectively.

Finally, the combined activation is applied as follow: the mixture of precursor-zinc chloride is treated in the same conditions as in the chemical activation (without landing of 1 h); the nitrogen is then switched to carbon dioxide for 1 h at 800°C. After cooling under a nitrogen stream, the resulting carbon is washed in the same conditions as in the chemical activation. We

shall note that CC1, CC2, and CC3, the precursors, were successively activated by 0.5, 1, and 2 g of $ZnCl_2$ per gram olive stones then by CO_2 for 1 h, respectively.

The yield of the activated carbon was estimated from the following equation:

$$\text{Yield of activated carbon (\%)} = \frac{\text{weight of activated carbon}}{\text{weight of dried olive stones}} \times 100 \quad (1)$$

2.2. Nitrogen adsorption–desorption and immersion calorimetry

The textural characterization of the prepared activated carbons was performed by nitrogen adsorption and immersion calorimetry techniques. The nitrogen adsorption–desorption isotherms were measured using an automatic adsorption volumetric apparatus (Micromeritics ASAP 2010) in order to determine the specific surface areas S_{BET} from the BET equation [34], the total pore volume (V_T) at a relative pressure of 0.98, and the micropore volume (W_0) from Dubinin–Radushkevich [35]. The mesopore volume (V_{meso}) was obtained by calculating the difference between the total volume and the micropore volume.

The microporosity was also studied by immersion calorimetry in a Setaram Tian-Calvet C80D calorimeter [33,36–38], using bulb method of fragile point, in two liquids (cyclohexane and tri-2,4-xilyl phosphate).

2.3. Phenol adsorption

2.3.1. Adsorption kinetics

Adsorption experiments were carried out using the batch method. For every phenol adsorption kinetics experiment, we introduce 0.05 g of activated carbon in a set of Erlenmeyer flasks; each one containing 50 mL of phenol solution of 150 mg/L. The initial pH of the phenol solution was controlled to 7.5 by adding 0.1 N HCl or 0.1 N NaOH solution dropwise. The mixture was agitated in a temperature-controlled shaking water bath (25°C), at a constant shaking speed of 120 rpm for different times. At the end of the reaction time, the content of each flask was filtered and the filtrate solution was analyzed on a UV-spectrophotometer (JASCO V-530) at 270 nm.

The amount of phenol adsorbed on the activated carbon at time t, q_t (mg/g), was calculated using the following relation:

$$q_t = \frac{(C_0 - C_t)}{m} V \quad (2)$$

where C_0 (mg/L), C_t (mg/L), V (L), and m (g) are the initial concentration of phenol, the equilibrium concentration of phenol at time t, the volume of phenol solution, and the mass of activated carbon, respectively.

The percentage removal of phenol was calculated by applying the following equation:

$$\%\ \text{Removal of phenol} = \frac{(C_i - C_e)}{C_i} \times 100 \quad (3)$$

2.3.2. Adsorption isotherms

The adsorption isotherms of phenol on various activated carbons are made at different phenol concentrations with a regular agitation for 24 h at 25°C. Such a time is indeed enough for reaching equilibrium. The amount of adsorbed phenol at equilibrium (q_e) was calculated according to the following equation:

$$q_e = \frac{(C_i - C_e)}{m} V \quad (4)$$

where C_i and C_e represent the initial concentration and the equilibrium phenol concentration, respectively.

3. Results and discussion

3.1. Characterization of the activated carbons

The nitrogen adsorption–desorption isotherms of various activated carbons corresponding to three modes of activation are represented in Figs. 1–3, respectively.

The textural parameters values of different activated carbons are summarized in Table 1. The values of the immersion enthalpies of the activated carbons

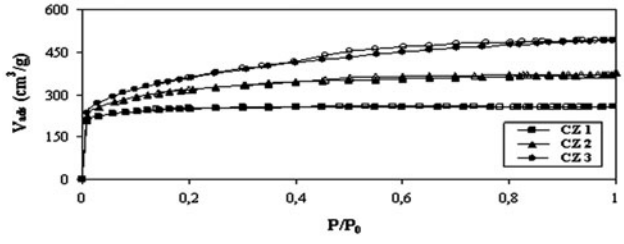

Fig. 1. Adsorption–desorption isotherms of N_2 on olive stones treated by different ratios of $ZnCl_2$ and carbonized for 1 h at 800°C.

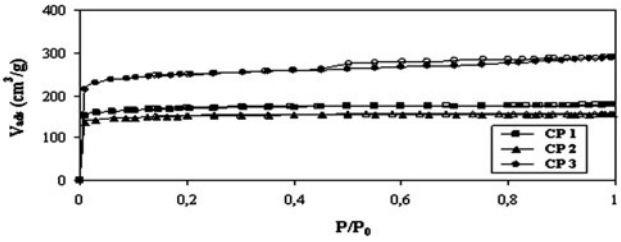

Fig. 2. Adsorption–desorption isotherms of N_2 on the olive stones physically activated by CO_2 for 1, 2, and 3 h at 800˚C.

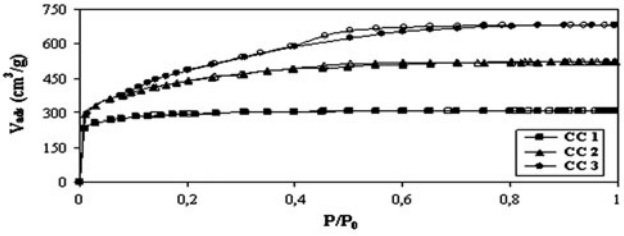

Fig. 3. Adsorption–desorption isotherms of N_2 on the olive stones chemically activated by different ratios of $ZnCl_2$ at 800˚C following by CO_2 activation for 1 h.

in cyclohexane [$-\Delta H_i$ (C_6H_{12})] and tri-2,4-xilyl phosphate [$-\Delta H_i$ ($C_{24}H_{27}O_4P$)] are given in the same table.

Figs. 1–3 show that adsorption–desorption isotherms of all nitrogen on various activated carbons are in type I, according to the classification of the IUPAC [39]; these materials are then essentially microporous, except for CZ3, CP3, and CC3 for which we observe an hysteresis loop of type H_4, a characteristic of capillary condensation phenomenon due to the presence of slit-like mesopores. We notice that the larger the ratio of $ZnCl_2$ to olive stones (coals CZ and CC) and the duration of preservation of CO_2 (coals CP), the more developed the porous texture.

Table 1 shows that the values of all the textural parameters (specific surface, porous volume, and average pores diameter) increase with the increasing ratio of $ZnCl_2$ as well in the cases of the chemical activation (coals CZ) and the combined activation (coals CC); it is important to note that this increase is more pronounced in the last case. Moreover, it is known that the zinc chloride alters the course of reactions in the carbonization so that less tarry products, responsible for blocking the enter of the pores, are formed; it was also showed that the porosity created is due to the spaces left by $ZnCl_2$ [2,40]; this is confirmed by the increasing values of immersion enthalpies in tri-2,4-xilyl phosphate, with the increasing ratio of $ZnCl_2$. Furthermore, the decrease of [$-\Delta H_i$ (C_6H_{12})] and the increase of [$-\Delta H_i$ ($C_{24}H_{27}O_4P$)] show that the average pores diameter becomes more and more larger because of the weak interactions of C_6H_{12} and the strong interactions of $C_{24}H_{27}O_4P$ with the pore wall, respectively. As to the activated carbons obtained by the physical activation (CP), they are essentially characterized by a microporous texture; similar results obtained on agricultural by-products activated by CO_2 [41,42]. It also should be noticed that combined activation leads to the coals characterized by the widest pores as shown in Fig. 4. This suggests that the micropores of CP3 are mostly larger pores. This result is confirmed by the great value of the immersion enthalpies in cyclohexane [$-\Delta H_i$ (C_6H_{12})]. Otherwise, it is interesting to notice that the best activated carbon, in terms of the porous texture, is the one obtained by the combined activation (CC3).

The yield of activated carbon during chemical and combined activations is higher than the yield obtained by the physical activation with CO_2 (Table 1). A

Table 1
Textural parameters of various activated carbons

Activated carbon	Yield (%)	S_{BET} (m^2/g)	V_T (cm^3/g)	W_0 (cm^3/g)	V_{meso} (cm^3/g)	W_0/V_T (%)	Φ (Å) = $4V_T/S_{BET}$	$-\Delta H_i$ (C_6H_{12}) (J/g)	$-\Delta H_i$ ($C_{24}H_{27}O_4P$) (J/g)
CZ1	55.8	834	0.39	0.38	0.015	96.50	18.70	63.32	–
CZ2	52.2	1,093	0.57	0.45	0.12	79.20	20.86	71.30	–
CZ3	48.6	1,266	0.76	0.49	0.26	65.00	24.01	76.81	–
CP1	40.1	563	0.27	0.26	0.01	96.00	19.18	23.76	–
CP2	35.8	520	0.24	0.23	0.006	97.50	18.46	9.47	–
CP3	34.7	861	0.44	0.38	0.06	86.50	20.44	150.70	–
CC1	50.4	985	0.47	0.44	0.03	93.30	19.08	91.76	2.10
CC2	45.6	1,546	0.81	0.60	0.21	74.20	20.96	28.13	76.13
CC3	44.1	1,793	1.05	0.68	0.37	64.70	23.42	29.32	170.79

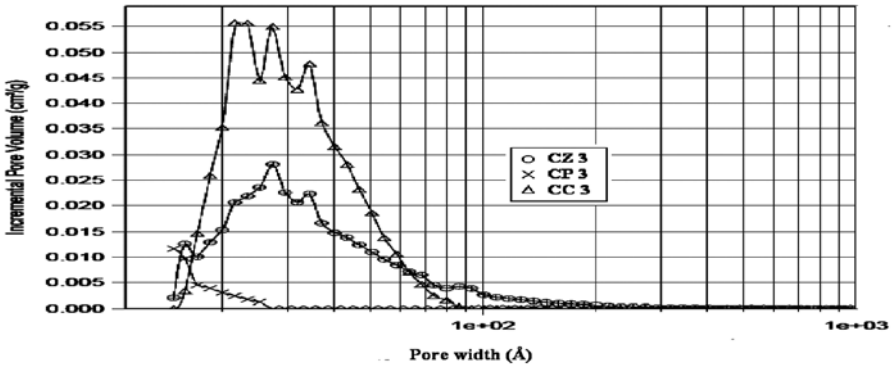

Fig. 4. Pore size distribution of CZ3, CP3, and CC3.

combined activation was found to yield carbon material (CC3) at 44.1 wt.% with a high specific surface area value of 1,793 m^2/g. Lastly, for a same series of prepared activated carbons, the variation of the total pore volume V_T according to the rate of $ZnCl_2$ or the CO_2 flow is linear; this is probably due to a continuous development of the porous texture.

3.2. Phenol adsorption study

3.2.1. Adsorption kinetics of phenol

The adsorption kinetics of phenol on various activated carbons obtained by the chemical, physical, and combined activations are represented in Figs. 5–7, respectively.

These figures show that the quantity of the adsorbed phenol increases with contact time. The phenomenon of phenol adsorption is practically instantaneous; indeed, the saturation of the coal surface is very quickly reached; this denotes a big affinity between the activated carbon and the molecules of the phenol.

In order to investigate the adsorption process of phenol onto different activated carbons, the kinetic models such as the pseudo-first-order and pseudo-second-order reaction rate equations are used.

The pseudo-first-order kinetic model [43] can be written in the following form:

$$\ln(q_e - q_t) = \ln(q_e) - k_1 t \quad (5)$$

where q_e (mg/g) and q_t (mg/g) are the amounts of phenol adsorbed at equilibrium and at time t (min), respectively and k_1 (min^{-1}) is the adsorption rate constant of the pseudo-first-order model.

The k_1 and q_e values were evaluated from the slope and intercept of the linear plots of $\ln(q_e - q_t)$ vs. t, respectively.

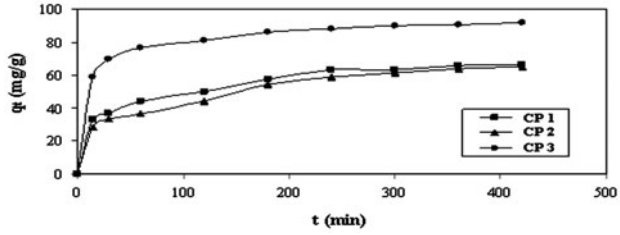

Fig. 6. Adsorption kinetics of phenol on activated carbons obtained by physical activation.

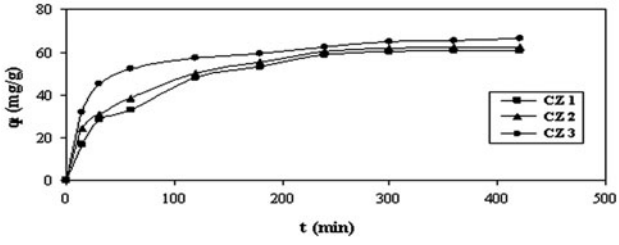

Fig. 5. Adsorption kinetics of phenol on activated carbons obtained by chemical activation.

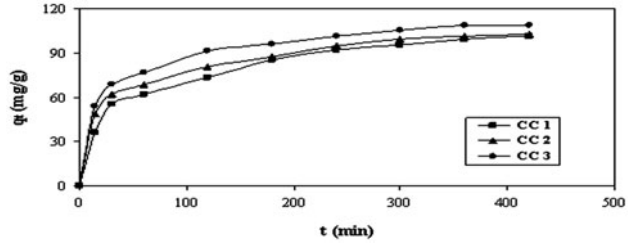

Fig. 7. Adsorption kinetics of phenol on activated carbons obtained by combined activation.

Table 2
Comparison of the first- and second-order constants for the phenol adsorption on different activated carbons

Activated carbon	q_e (mg/g) (experimental)	First-order kinetic model			Second-order kinetic model		
		$K_1 \times 10^3$ (min^{-1})	q_e (mg/g) (calculated)	R^2	$K_2 \times 10^4$ ($g\,mg^{-1}\,min^{-1}$)	q_e (mg/g) (calculated)	R^2
CZ1	61.00	13.82	61.16	0.985	2.87	68.97	0.998
CZ2	62.36	17.27	73.79	0.943	3.86	68.49	0.998
CZ3	66.52	8.75	30.28	0.975	6.98	68.97	0.999
CP1	66.30	10.59	45.41	0.958	4.35	70.92	0.996
CP2	65.07	9.21	49.45	0.963	3.08	70.92	0.990
CP3	91.87	9.21	31.33	0.992	7.88	94.34	0.999
CC1	101.39	8.98	72.28	0.978	2.16	109.89	0.996
CC2	102.40	10.59	70.10	0.951	2.98	108.70	0.996
CC3	108.85	8.98	57.68	0.986	3.36	114.94	0.998

The pseudo-second-order model [44] can be represented in the following form:

$$\frac{t}{q_t} = \frac{1}{k_2 q_e^2} + \frac{t}{q_e} \tag{6}$$

The amounts of phenol adsorbed at equilibrium q_e (mg/g) and the rate constant of the pseudo-second-order model k_2 ($g\,mg^{-1}\,min^{-1}$) values can be determined experimentally from the slope and intercept of the linear plots of t/q_t vs. t, respectively.

The kinetic parameters from Eqs. (3) to (4) are shown in Table 2.

The analysis of the R^2 values for phenol adsorption on different activated carbons shown in Table 2 suggests that the experimental data fit the pseudo-second-order model with R^2 values greater than 0.990 than those of the pseudo-first-order model with R^2 values ranging between 0.943 and 0.992. It can be seen that the pseudo-second-order kinetic model better represents the adsorption kinetics and the calculated q_e values agree well with the experimental q_e values (Table 2). The best fit to the pseudo-second-order kinetics indicates that the adsorption mechanism depends on the phenol and activated carbon.

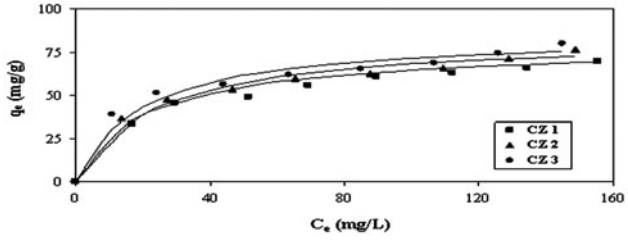

Fig. 8. Adsorption isotherms of phenol on activated carbons obtained by chemical activation.

3.2.2. Phenol adsorption isotherms

The adsorption isotherms of phenol on different activated carbons are represented in Figs. 8–10.

The phenol adsorption isotherms for all activated carbons indicated that the amount of phenol adsorbed increased with increasing equilibrium concentration. The results were analyzed using the Langmuir and Freundlich models.

The Langmuir adsorption isotherm assumes monolayer adsorption on a completely homogeneous surface with negligible interactions between adsorbed molecules. The Langmuir [45] model is the most widely used isotherm equation, which has the following form:

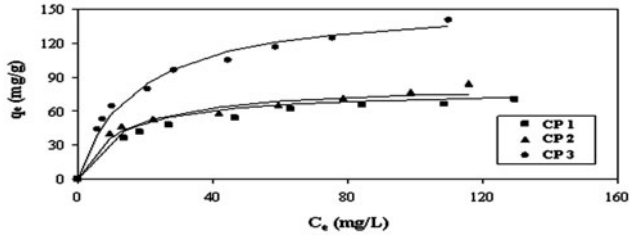

Fig. 9. Adsorption isotherms of phenol on activated carbons obtained by physical activation.

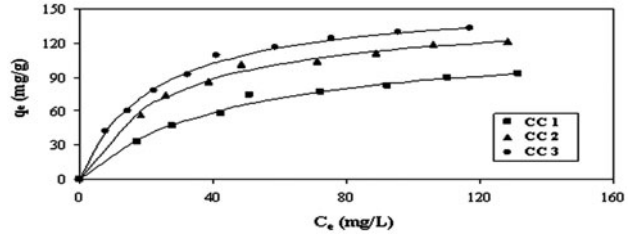

Fig. 10. Adsorption isotherms of phenol on activated carbons obtained by combined activation.

Table 3
Langmuir and Freundlich constants for the phenol adsorption on different activated carbons

Activated carbon	Langmuir model			Freundlich model		
	Q_0 (mg/g)	K_L (L/mg)	R^2	K_F (mg/g) (L/mg)$^{1/n}$)	n	R^2
CZ1	78.74	0.0449	0.992	14.92	3.26	0.971
CZ2	84.03	0.0421	0.986	17.74	3.50	0.988
CZ3	85.47	0.0500	0.983	21.48	3.91	0.982
CP1	78.74	0.0837	0.997	18.01	3.49	0.978
CP2	83.33	0.0791	0.990	22.88	3.79	0.981
CP3	156.25	0.0578	0.992	24.79	2.63	0.980
CC1	126.58	0.0216	0.988	8.74	1.99	0.948
CC2	147.06	0.0371	0.995	21.50	2.71	0.931
CC3	158.73	0.0451	0.999	19.67	4.07	0.957
CAC2	73.91	0.100	1.00	24.64	4.69	0.97
CAC3	137.36	0.130	1.00	33.77	3.07	0.94

$$q_e = \frac{Q_0 K_L C_e}{1 + K_L C_e} \tag{7}$$

The linear transformed form of Langmuir equation is given as:

$$\frac{C_e}{q_e} = \frac{1}{K_L Q_0} + \frac{C_e}{Q_0} \tag{8}$$

The maximum adsorption capacity Q_0 (mg/g) corresponding to complete monolayer coverage and the Langmuir isotherm constant K_L (L/mg) are determined by plotting $\frac{C_e}{q_e}$ vs. C_e.

The Freundlich empirical equation [46] has been proposed to fit adsorption data:

$$q_e = K_F C_e^{1/n} \tag{9}$$

The linear form of the Freundlich equation is given as:

$$\ln q_e = \ln K_F + \frac{1}{n} C_e \tag{10}$$

The Freundlich constant K_F (mg/g)/(L/mg)$^{1/n}$ and the heterogeneity factor ($1/n$) can be determined from the intercept and slope of the linear plot of ln(q_e) vs. ln(C_e), respectively.

The parameters values of the Langmuir and Freundlich models for the phenol adsorption on different activated carbons are listed in Table 3.

From these results, one observes that the maximal of phenol adsorption capacity, Q_0, is more raised on combined activation coals (CC1, CC2, and CC3) and on the CO_2 (3 h) activation coal CP3; this can be explained by the development more important of the porous textures (average pores diameter) during the activation process. Indeed, the values of Q_0 corresponding to activated carbons CP3 and CC3 are 156.5 and 158.7 mg/g respectively. It is interesting to notice that the two values are very close although the specific surface area (S_{BET}) of CP3 (861 m^2/g) is much lower than that of CC3 (1,793 m^2/g); this should be due to the presence of more narrow microporosity in the activated carbons CC3, this narrower microporosity being inaccessible to the phenol molecule. In addition, as is well known [47], the adsorption of phenol on activated carbons is based on the formation of donor–acceptor complexes between the surface carbonyl groups (electron donors) and the aromatic rings of phenol acting as the acceptor. As the activation by the carbon dioxide supports the formation of the carbonyl groups [2,42], the concentration of these latter would be higher in the case of physical activation than in that of combined activation; then, the quantity of adsorbed phenol is relatively important for CP3 even if its specific surface area is lower than that of CC3. The same remark can be made about the activated carbons CZ1 and CP3 which are characterized by very close specific surface areas (834 and 861 m^2/g respectively) but clearly differ by the phenol adsorption capacities (78.7 and 156.2 mg/g, respectively). These results show that there no correlation between phenol uptake and total specific surface area as they already reported by Terzyk [48]. Otherwise, for a same series, particularly for the series CC, the variation of the phenol adsorption capacity, Q_0, according the total pore volume V_T, is linear; this is probably

Table 4
Comparison of phenol adsorption capacities of various activated carbons

Adsorbents	S_{BET} (m^2/g)	Q_0 (mg/g)	References
CP3	861	156.25	This work
CC2	1,546	147.06	This work
CC3	1,793	158.73	This work
Commercial activated carbon (CAC1)	1,350	104.82	[23]
Commercial activated carbon (CAC2)	620	73.91	[23]
Commercial activated carbon (CAC3)	1,020	137.36	[23]
Coconut shell-based activated carbon	1,026	205.842	[49]
Avocado kernel seeds activated carbon	206	90	[50]
Activated carbon fibers	920.3	102.47	[51]

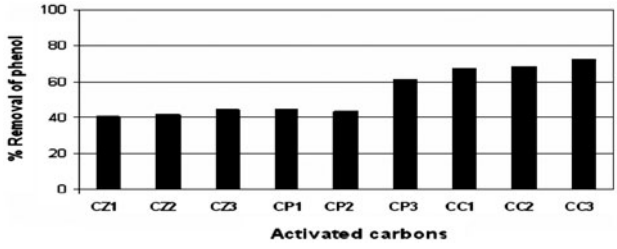

Fig. 11. Removal efficiency of phenol onto the activated carbons prepared by different methods ($C_0 = 150$ mg/L, contact times = 48 h, pH = 7.5, and temperature = 25°C).

due to a continuous development of the porous texture.

The value of n for Freundlich isotherm was found higher than unity, indicating that the phenol is favorably adsorbed by different activated carbons. According to the R^2 values, the Langmuir model fitted the experimental data is better than the Freundlich model.

Table 4 compares the phenol adsorption capacities of activated carbon obtained in this study to those of various activated carbons reported in literature.

From Table 4, it can be said that the prepared activated carbons from olive stones have comparable results of phenol adsorption performance with the others; in the most cited cases, they are more efficient. Also, the highest Q_0 values from this study are larger than the previous results (Table 4). These experimental results indicated that the olive stones, an agricultural waste, can be utilized for the production of activated carbons for the treatment of water contaminated with phenols. Indeed, the rate of the elimination of phenol from water corresponding to these activated carbons, particularly the activated carbon obtained by physicochemical activation (CC3), can reach 73% (Fig. 11).

4. Conclusion

An agricultural waste, olive stones, investigated in this work can be used as precursors to produce activated carbons characterized by a developed porous texture. Indeed, the specific surface area and the total pore volume of the activated carbon obtained by the combined activation (CC3) reach 1,793 m^2/g and 1.05 cm^3/g, respectively. The phenol adsorption capacity on these activated carbons is significant, especially in the cases of the physical activation by the carbon dioxide and the combined activation, i.e. the chemical activation by the zinc chloride following by the physical activation by CO_2; in this latter case, the adsorption capacity of CC3 reaches 158.7 mg/g. This value is comparable to commercial activated carbons and other adsorbents reported in earlier studies. The kinetics of phenol adsorption on the olive stones treated by $ZnCl_2$, CO_2, and $ZnCl_2$ followed by CO_2 successively are well described by the pseudo-second-order model. Furthermore, the isotherms of phenol adsorption on the same activated carbons perfectly fit Langmuir equation. From this study, it can be concluded that activated carbons produced from an agricultural waste, the olive stones, seem an effective alternative for the removal of phenol from aqueous solutions (the rate of elimination of phenol from water being relatively higher), because of its very developed porous texture (high specific surface area and high total pore volume), i.e. adsorption capacity, and low cost.

References

[1] F. Rodríguez-Reinoso, M. Molina-Sabio, Activated carbons from lignocellulosic materials by chemical and/or physical activation: An overview, Carbon 30(7) (1992) 1111–1118.
[2] Z. Hu, M.P. Srinivasan, Y. Ni, Novel activation process for preparing highly microporous and mesoporous activated carbons, Carbon 39(6) (2001) 877–886.

[3] M. Molina-Sabio, F. Rodríguez-Reinoso, F. Caturla, M.J. Sellés, Development of porosity in combined phosphoric acid-carbon dioxide activation, Carbon 34(4) (1996) 457–462.
[4] Z. Hu, E.F. Vansant, A new composite adsorbent produced by chemical activation of elutrilithe with zinc chloride, J. Colloid Interface Sci. 176(2) (1995) 422–431.
[5] A. Ahmadpour, D.D. Do, The preparation of active carbons from coal by chemical and physical activation, Carbon 34(4) (1996) 471–479.
[6] M. Molina-Sabio, F. Rodríguez-Reinoso, Role of chemical activation in the development of carbon porosity, Colloids Surf. A: Physicochem. Eng. Asp. 241 (2004) 15–25.
[7] M. Uğurlu, A. Gürses, M. Açıkyıldız, Comparison of textile dyeing effluent adsorption on commercial activated carbon and activated carbon prepared from olive stone by $ZnCl_2$ activation, Micropor. Mesopor. Mater. 111 (2008) 228–235.
[8] D.C.S. Azevedo, J.C.S. Araujo, M. Bastos-Neto, A.E.B. Torres, E.F. Jaguaribe, C.L. Cavalcante, Microporous activated carbon prepared from coconut shells using chemical activation with zinc chloride, Micropor. Mesopor. Mater. 100 (2007) 361–364.
[9] M.J. Prauchner, F. Rodriguez-Reinoso, Chemical vs. physical activation of coconut shell: A comparative study, Micropor. Mesopor. Mater. 152 (2012) 163–171.
[10] C. Zhang, Y. Wang, X. Yan, Liquid-phase adsorption: Characterization and use of activated carbon prepared from diosgenin production residue, Colloids Surf. A: Physicochem. Eng. Asp. 280 (2006) 9–16.
[11] S. Yorgun, N. Vural, H. Demiral, Preparation of high-surface area activated carbons from Paulownia wood by $ZnCl_2$ activation, Micropor. Mesopor. Mater. 122 (2009) 189–194.
[12] F.C. Wu, R.L. Tseng, High adsorption capacity NaOH-activated carbon for dye removal from aqueous solution, J. Hazard. Mater. 152 (2008) 1256–1267.
[13] H. Marsh, D.S. Yan, T.M. O'Grady, A. Wennerberg, Formation of active carbons from cokes using potassium hydroxide, Carbon 22 (1984) 603–611.
[14] P. Ehrburger, A. Addoun, F. Addoun, J.B. Donnet, Carbonization of coals in the presence of alkaline hydroxides and carbonates: Formation of activated carbons, Fuel 65 (1986) 1447–1449.
[15] F.C. Wu, P.H. Wu, R.L. Tseng, R.S. Juang, Preparation of activated carbons from unburnt coal in bottom ash with KOH activation for liquid-phase adsorption, J. Environ. Manage. 91 (2010) 1097–1102.
[16] A. Addoun, J. Dentzer, P. Ehrburger, Porosity of carbons obtained by chemical activation: Effect of the nature of the alkaline carbonates, Carbon 40 (2002) 1140–1143.
[17] J.S. Mattson, Jr., H.B. Mark, Activated Carbon: Surface Chemistry and Adsorption from Solution, Marcel Dekker, New York, NY, 1971.
[18] T.M. Alslaibi, I. Abustan, M.A. Ahmad, A. Abu Foul, Review: Comparison of agricultural by-products activated carbon production methods using surface area response Caspian, J. Appl. Sci. Res. 2 (2013) 18–27.
[19] P.G. González, Y.B. Pliego-Cuervo, Physicochemical and microtextural characterization of activated carbons produced from water steam activation of three bamboo species, J. Anal. Appl. Pyrolys. 99 (2013) 32–39.
[20] T.M. Alslaibi, I. Abustan, M.A. Ahmad, A. Abu Foul, Application of response surface methodology (RSM) for optimization of Cu^{2+}, Cd^{2+}, Ni^{2+}, Pb^{2+}, Fe^{2+}, and Zn^{2+} removal from aqueous solution using microwaved olive stone activated carbon, J. Chem. Techn. Biotechn. (in press), doi: 10.1002/jctb.4073.
[21] K. László, E. Tombácz, C. Novák, pH-dependent adsorption and desorption of phenol and aniline on basic activated carbon, Colloids Surf. A: Physicochem. Eng. Asp. 306 (2007) 95–101.
[22] I.P.P. Cansado, P.A.M. Mourão, A.I. Falcão, M.M.L. Ribeiro Carrott, P.J.M. Carrott, The influence of the activated carbon post-treatment on the phenolic compounds renoval, Fuel Process. Technol. 103 (2012) 64–70.
[23] V. Fierro, V. Torne-Fernandez, D. Montane, A. Celzard, Adsorption of phenol onto activated carbons having different textural and surface properties, Micropor. Mesopor. Mater. 111 (2008) 276–284.
[24] B.H. Hameed, A.A. Rahman, Removal of phenol from aqueous solutions by adsorption onto activated carbon prepared from biomass material, J. Hazard. Mater. 160 (2008) 576–581.
[25] C.W. Purnomo, C. Salim, H. Hinode, Effect of the activation method on the properties and adsorption behavior of bagasse fly ash-based activated carbon, Fuel Process. Technol. 102 (2012) 132–139.
[26] A. Kumar, S. Kumar, D.V. Gupta, Adsorption of phenol and 4-nitrophenol on granular activated carbon in basal salt medium: Equilibrium and kinetics, J. Hazard. Mater. 147 (2007) 155–166.
[27] J. Silvestre-Albero, A. Silvestre-Albero, F. Rodriguez-Reinoso, M. Thommes, Physical characterization of activated carbons with narrow microporosity by nitrogen (77.4 K), carbon dioxide (273 K) and argon (87.3 K) adsorption in combinaison with immersion calorimetry, Carbon 50(9) (2012) 3128–3133.
[28] T.A. Centoro, J.A. Fernandez, F. Stoeckli, Correlation between heats of immersion and limiting capacitances in porous carbons, Carbon 46(7) (2008) 1025–1030.
[29] E. Castillejos, B. Bachiller, I. Rodriguez-Ramos, A. Guerrero-Ruiz, An immersion calorimetry study of the interaction of organic compounds with carbon nanotube surfaces, Carbon 50(8) (2012) 2731–2740.
[30] F. Stoeckli, T.A. Centeno, On the determination of surface areas in activated carbons, Carbon 43 (2005) 1184–1190.
[31] F. Stoeckli, A. Guillot, A.M. Slasli, D. Hugi-Cleary, The comparaison of experimental and calculated pore size distributions of activated carbons, Carbon 40 (2002) 383–388.
[32] E. Sheng, I. Sutherland, R.H. Bradley, P.K. Freakley, Heat of immersion calorimetry studies of carbon blacks, Mater. Chem. Phys. 50 (1997) 25–30.
[33] F. Rodríguez-Reinoso, M. Molina-Sabio, M.T. González, Effect of oxygen surface groups on the immersion enthalpy of activated carbons in liquids of different polarity, Langmuir 13(8) (1997) 2354–2358.
[34] S. Brunauer, P.H. Emmett, E. Teller, Adsorption of gases in multimolecular layers, J. Am. Chem. Soc. 60(2) (1938) 309–319.
[35] M.M. Dubinin, Progress in Surface and Membrane Science, Academic Press, London, (J.W. Patrick) 1975.
[36] R. Denoyel, J. Fernandez-Colina, Y. Grillet, J. Rouquerol, Assessment of the surface area and microporosity of activated charcoals from immersion calorimetry and nitrogen adsorption data, Langmuir 9 (1993) 515–518.
[37] J. Silvestre-Albero, C. Gómez de Salazar, A. Sepúlveda-Escribano, F. Rodríguez-Reinoso, Characterization of microporous solids by immersion calorimetry, Colloids Surf. A: Physicochem. Eng. Asp. 187–188 (2001) 151–165.
[38] H.F. Stoeckli, F. Kraehenbuehl, The enthalpies of immersion of active carbons, in relation to the Dubinin theory for the volume filling of micropores, Carbon 19 (1981) 353–356.
[39] K.S.W. Sing, D.H. Everett, R.A.W. Haul, L. Moscou, R.A. Pierotti, J. Rouquerol, T. Siemieniewska, Reporting physisorption data for gas/solid systems with special reference to the determination of surface area and porosity, Pure Appl. Chem. 57 (1985) 603–619.
[40] F. Caturla, M. Molina-Sabio, F. Rodriguez-Reinoso, Preparation of activated carbon by chemical activation with $ZnCl_2$, Carbon 29(7) (1991) 999–1007.
[41] J. Rivera-Utrilla, C. Moreno-Castilla, M.V. Lopez-Ramon, F. Carrasco-Marin, M.A. Ferro-Garcia, Activated carbons from coals and agricultural by-products as adsorbents in aqueous phase: Preparation, characterization and adsorption of phenolic compounds under static and dynamic conditions, Curr. Topic. Colloid Interface Sci. 1 (1997) 51–67.
[42] M. Belhachemi, Z. Belala, D. Lahcene, F. Addoun, Adsorption of phenol and dye from aqueous solution using chemically modified date pits activated carbons, Desalin. Wat. Treat. 7 (2009) 182–190.

[43] S. Lagergren, Zur theorie der sogenannten adsorption geloester stoffe [About theory of so-called adsorption of soluble substances], Kungliga Svenska Vetenskapsakademiens Handl. 24 (4) (1898) 1–39.
[44] Y.S. Ho, G. McKay, Sorption of dye from aqueous solution by peat, Chem. Eng. J. 70 (1998) 115–124.
[45] I. Langmuir, The adsorption of gases on plane surfaces of glass, mica and platinum, J. Am. Chem. 57 (1918) 1361–1403.
[46] H.M.F. Freundlich, Adsorption in solution, J. Phys. Chem. 57 (1906) 384–470.
[47] J.S. Mattson, H.B. Mark, Activated Carbon. Surface Chemistry and Adsorption from Solution, Marcel Dekker, New York, NY, 1971.
[48] A.P. Terzyk, Further insights into the role of carbon surface functionalities in the mechanism of phenol adsorption, J. Colloid Interface Sci. 268 (2003) 302–329.
[49] A.T.M. Din, B.H. Hameed, A.L. Ahmad, Batch adsorption of phenol onto physiochemical-activated coconut shell, J. Hazard. Mater. 161 (2009) 1522–1529.
[50] L.A. Rodrigues, M.L.C.P.D Silva, M.O. Alvarez-Mendes, A.D. R. Coutinho, G.P. Thim, Phenol removal from aqueous solution by activated carbon produced from avocado kernel seeds, Chem. Eng. J. 174 (2011) 49–57.
[51] Q.S. Liu, T. Zheng, P. Wang, J.P. Jiang, N. Li, Adsorption isotherm, kinetic and mechanism studies of some substituted phenols on activated carbon fibers, Chem. Eng. J. 157 (2010) 348–356.